IEEE Access
Multidisciplinary | Rapid Review | Open Access Journal

Received July 20, 2019, accepted August 15, 2019, date of publication August 26, 2019, date of current version September 12, 2019.

Digital Object Identifier 10.1109/ACCESS.2019.2937624

MR Fully Compatible and Safe FBG Breathing Sensor: A Practical Solution for Respiratory Triggering

MARCEL FAJKUS[1], JAN NEDOMA[1], RADEK MARTINEK[2], JINDRICH BRABLIK[2], JAN VANUS[2], MARTIN NOVAK[1], STANISLAV ZABKA[1], VLADIMIR VASINEK[1], PAVLA HANZLIKOVA[3], AND LUBOMIR VOJTISEK[4]

[1]Department of Telecommunications, Faculty of Electrical Engineering and Computer Science, VSB—Technical University of Ostrava, 708 00 Ostrava, Czech Republic
[2]Department of Cybernetics and Biomedical Engineering, Faculty of Electrical Engineering and Computer Science, VSB—Technical University of Ostrava, 708 00 Ostrava, Czech Republic
[3]Department of Imaging Methods, Faculty of Medicine, University of Ostrava, 701 03 Ostrava, Czech Republic
[4]Neuroscience Centre, Central European Institute of Technology (CEITEC), Masaryk University, 601 77 Brno, Czech Republic

Corresponding author: Marcel Fajkus (marcel.fajkus@vsb.cz)

This work was supported in part by the Ministry of Education of the Czech Republic under Project SP2019/80 and Project SP2019/85, in part by the Ministry of Education, Youth and Sports of the Czech Republic (MEYS CR) within the framework of the Operation Programme Education for Competitiveness financed by the European Structural Funds and from the State Budget of the Czech Republic under Grant CZ.1.07/2.3.00/20.0217, in part by the Ministry of the Interior of the Czech Republic under Project VI20152020008 and Project VI2VS/444, in part by the Ministry of Industry and Trade of the Czech Republic under Project FV10396 and Project FV20581, in part by the Grand Agency of the Czech Republic under Project 15-21547S, in part by the European Regional Development Fund in the Research Centre of Advanced Mechatronic Systems Project within the Operational Programme Research, Development and Education under Project CZ.02.1.01/0.0/0.0/16_019/0000867, in part by the European Regional Development Fund in Research Platform focused on Industry 4.0 and Robotics in Ostrava Project within the Operational Programme Research, Development and Education under Project CZ.02.1.01/0.0/0.0/17_049/0008425, and in part by the MEYS CR (Czech-BioImaging) under Grant LM2015062.

ABSTRACT This publication describes an original simple low-cost MR fully-compatible and safe fiber-optic breathing sensor (FOBS), which can be used for respiratory triggering and for monitoring the development of respiratory rate within the MR environment and can, thus, serve as prevention from the hyperventilation syndrome. The sensor is created by encapsulation of the Bragg grating into conventional nasal oxygen cannulas. The sensor is immune to minor patient movements, thus limiting movement artifacts to a minimum. Thanks to this fact it can be used for the retrospective/prospective respiratory gating. The sensor is immune to electromagnetic interference (EMI) and can thus be used in any magnetic field (1.5T, 3T, and 7T). The sensor prototype has been tested in both laboratory and real magnetic resonance (3T) environments relative to conventional pneumatic respiration references (PRR). The data measured were statistically evaluated using the objective Bland-Altman method (BAM) and the functionality of the proposed solution was confirmed. Respiratory Triggering functionality was confirmed by the radiologic doctors on the basis of analyzing images using the most used respiratory triggered T2 TSE 3D sequences and by objective method using the Blind/Referenceless Image Spatial Quality Evaluator (BRISQUE).

INDEX TERMS Magnetic resonance imaging (MRI), respiratory rate (RR), fiber-optic sensor, fiber Bragg grating (FBG), respiratory triggering.

I. INTRODUCTION

Patients undergoing MRI independent of magnetic field strength should be monitored during the examination - vital functions monitoring. The basic parameters monitored include heart rate (HR) and respiratory rate (RR) of a human body. The development of these vital functions over time for diagnosis purposes in case of mild, but also more serious complications, is used as a basic tool for problem situation diagnosis. The most widespread problem situations that arise within MRI include hyperventilation syndrome [1], [2]. In the case of magnetic resonance, the hyperventilation syndrome is most often caused by the closed so-called tunnel environment of the scanner. It is a condition primarily related to breathing activity when the patient starts breathing rapidly. As a result

The associate editor coordinating the review of this article and approving it for publication was Wei Wei.

of the accelerated release of carbon dioxide (whose compounds form a significant proportion of the natural pH correction), the body loses acid-base balance–blood pH increases, resulting in so-called respiratory alkalosis (change in bicarbonate and carbonic acid concentration ratios). The human body tries to neutralize respiratory alkalosis, thus beginning to release H^+ (hydrogen cations) from the cells. As a result, Ca_2^+ ions (calcium) will bond, so free calcium deficiency begins to occur in the body. This process triggers the symptoms of hyperventilation tetany. Physically, hyperventilation syndrome manifests itself on the patient's body as prickling, tingling, both on the tips of the limbs and throughout the body. Strong spasms can gradually appear throughout the body, the patient may be disoriented and irritated. Hyperventilation tetany may last in a matter of minutes or hours and may lead to life-threatening conditions [3], [4].

Therefore, in MRI medical indications, it is advisable to monitor the development of the pulse or respiratory rate over time. As for respiration reference, pneumatic respiration transducers are the most commonly used clinically today [5]–[7]. These are relatively reliable devices supplied by different manufacturers. However, their disadvantage is the fact that the signal measured may be degraded when the patient moves. What is also important is that in the case of bigger patients, proper attachment of the device to the patient's body may be problematic; because of the proper tension, the belt must be stretched around the body. Also, correct tension adjustment of the respiration transducer is important for achieving the best sensitivity; it is often necessary to clamp the respiration belt repeatedly to achieve the desired sensitivity.

Conventional reference devices for recording physiological parameters, such as the respiration curve as well as ECG, also have benefits in the form of retrospective 'cleaning - filtration' within fMRI studies and diffusion data on respiration effects. However, if the subject tested in the MR scanner moves more than normal respiration activity is, it causes additional noise-artifacts that are very difficult to eliminate and their impact on the measured data evaluation is hard to assess. This results in a deterioration of the recording, or the recording needs to be repeated [8].

This publication focuses on an alternative approach in the form of fiber-optic technology that is an appropriate alternative to the MRI environment, as stated below, and can address the above-stated issues. This publication is also one of the first studies to provide a description and functional implementation of respiratory triggering by the pure fiber-optic technology.

II. STATE OF THE ART

There are several studies that have described the use of fiber-optic technology to monitor the respiratory rate of the human body. The basis here consists of interferometric and grating sensors. In the case of interferometric sensors, the most interesting publications include [9], where Podbreznik et al. presented cost-efficient speckle interferometry with plastic optical fiber for unobtrusive monitoring of human vital functions. The system is based on speckle interferometry; the results were analysed by means of 10 healthy persons in the supine position. Based on the results, the authors assessed the accuracies of 98.8 % ±1.5 % and 97.9 % ±2.3 % and the sensitivities of 99.4 % ±0.6 % and 95.3 % ±3 % for the heartbeat and respiration are obtained respectively. Favero *et al.* [10] presented a microstructured optical fiber interferometric respiration sensor which consists of a section of photonic crystal fiber (PCF) fusion spliced at the distal end of a standard telecommunication optical fiber. The sensor proposed can be used to monitor a person's breathing whatever the respiration rate is. The use of interferometric sensors for monitoring respiratory rate is very closely addressed by Sprager *et al.* [11], [12], and [15], Sprager and Zazula [13], and Zazula and Sprager [14], where for example publication [15] describes a sensor for unobtrusive and continuous monitoring of a person's vital functions. The sensor performed with the optical fiber on the mattress. The statistics is based on the data acquired from 5 male persons in the duration of about 60 s. As for respiration, the results obtained indicated a sensitivity of 93.8 %. In the article [16], the authors described an interferometric sensor for monitoring respiratory and heart rates of the human body. They used a Mach-Zehnder interferometer. The measuring part (fiber) was encapsulated into a thin circular layer made of polyurethane. Based on the Bland-Altman analysis, the authors defined accuracy for the respiratory rate averaging 96.49 %. The authors of [17] presented an optical respiration sensor based on an agarose infiltrated photonic crystal fiber interferometer. The interferometer is part of a respirator mask that is placed on the patient's mouth. The sensor detects the variation in relative humidity that occurs between the inhale and exhale. The sensor is suitable for monitoring patients during the MRI. The summaries of the use of the fiber - optic interferometer for biomedical applications are very well described in [18]–[20].

In the case of fiber Bragg grating sensors (FBG), the most interesting publications include [21], where the authors present a prototype of a fiber-optic sensor for recording the ballistocardiographic signal during MRI. The sensor was tested in both laboratory and real conditions during an MRI examination. The sensor is created by glueing the FBG with epoxy adhesive to a plexiglass plate with dimesions of 95×220 mm and a thickness of 1.5 mm was used. Based on the results, 96 % of the samples recorded lie within a ±1.96 SD range (standard deviation range) and no significant differences between the individuals were observed. The article [22] describes three MRI compatible respiration sensors based on fiber Bragg gratings, optical time-domain reflectometry, and macro-bending effects. The developed smart medical textiles can sense elongation of up to 3 % while maintaining the stretching properties of the textile substrates for patient's comfort. The sensors were tested in a MR environment and on healthy adults. Dziuda *et al.* [23] described a sensor based on the FBG which was encapsulated on a

plexiglass board. The results were obtained from a patient during real MRI. The statistic is based on three patients; the authors reported that 95.38 % and 94.88 % of the data lied within the LoA (Limit of Agreement) of the range for the respiratory rate 0.85 rpm (respiratory per minute) and heart rate 3.29 bpm (beat per minute) determinations respectively. The relative error level was below 8 %. The article [24] described a sensor head which consists of an FBG attached to an elastic board placed between the monitored person's body and a soft surface, enabling the board to deform in an unobstructed way. Tests carried out in the MRI environment proved the method to be immune to strong electromagnetic fields. An RMS value of the relative error was below 1.8 %. Nedoma *et al.* [25] designed and created a sensor based on an FBG probe encapsulated inside fiberglass (fiberglass is a composite material consisting of glass fiber, fabric, and cured synthetic resin). The sensor is characterized by small dimensions ($30\times10\times0.8$ mm) and low weight (2 g). The sensor was tested in real MRI and is characterized for RR by a relative error below 5 %. Leal-Junior *et al.* [26] present development of a polymer optical fiber sensor for simultaneous measurement of respiratory and heart rates. The sensor is embedded as a smart textile solution that can be used in the user's clothes. The results show errors below 4 beats per minute and 2 breaths per minute for the HR and BR respectively. An overview of the fiber-optic technology used in real MR environments is reported in the article [27]. A total of 47 MR-tested or potentially MR-compatible sensors have been described, but no sensor has been encapsulated in nasal oxygen cannulas (Medical adult soft nasal oxygen cannula tube for oxygen concentrator, Marne Medical, Australia).

CMRI (cardiac MRI) can be performed with a majority of measurements, in a state where the patient is not breathing or holding their breath, specifically due to the reduction of the aforementioned breathing-induced movement artifacts. This fact is, however, limited by the scanning time to about 15–25 seconds. Breath retention must be longer because one plane is picked up for several cardiac cycles. In clinical practice, it limits the examination of many patients (especially elderly and sick people). Respiratory triggering for MRI during free breathing is primarily designed to scan the abdomen and chest when pneumatic respiratory belts are used. Navigation (NAV) echoes (an additional RF pulse capable of detecting the position of the diaphragm and, thus, its movement in order to monitor the diaphragm position) is a modern approach to respiratory triggering [28], [29]. NAVs allow acquisition during a short sampling window at each cardiac cycle. The NAV echo is acquired immediately after the acquisition window, which means that there is a short time interval between the acquisition of the navigation echo and the acquisition of the image data. Nevertheless, when scanning with CMRI, data needs to be captured throughout the cardiac cycle, so triggering with one navigation echo within one cycle is insufficient for this purpose. For this reason, it is advantageous to use the self-gating method that allows both cardiac and respiratory activity to be triggered. This method is, however, based on a complicated correlation calculation between the triggering image and the target image obtained at the same cardiac phase and the desired position of the respiratory cycle [29], [30].

Within cardiac/respiratory triggering methods by pure fiber-optic technology, there are only some studies, which investigated the possibility of sensing cardiac or respiratory activity by optical fiber, but only when used in rodents [31]. The sensor is orally introduced into the rat's oesophagus or is placed on the chest the movement of which it senses [32]. In our previous research [25], we discussed the novel fiber Bragg grating probe encapsulated inside fiberglass. We analyzed the time span of the R–J ranged from 121–143 ms which is needed for cardiac triggering, but the practical research of cardiac triggering is still performed.

The authors see the benefits to this publication in the presentation of an original low-cost (more in the discussion) MR-compatible To demonstrate the functionality of the respiratoryfiber Bragg Grating (FBG) sensor, which can be used to reliably monitor the development of respiratory rate reliably even under high magnetic field conditions. The sensor is created by innovative encapsulation of the Bragg grating into conventional nasal oxygen cannulas. Due to the innovative encapsulation, the sensor is immune to random patient movements (minor movements of the patients do not affect the measuring signal). Thanks to this, the sensor presented can be used for the retrospective 'cleansing' of the fMRI and diffusion data on the effect of cardiac activity and breathing, as well as for respiratory triggering - synchronization of MR signal to the respiratory cycle (more in the discussion). For the scan, the imaging of the upper abdomen and the lower chest requires minimum diaphragm movement. When imaging of organs of the abdominal cavity or thoracic currently most frequently used semence with apnoea, which can take up to 25 seconds (time limit of one inspiration). If a longer sequence is needed and cannot be shortened to preserve spatial information, it is necessary to use breath monitoring [33]; however, not every sequence allows breath monitoring to be included in the current software equipment of the scanner. The authors see a potential benefit in the development of sequences using reliable and cheap breath monitoring. The sensor is immune to electromagnetic interference (EMI) and can thus be used in any magnetic field (1.5T, 3T and 7T). The sensor prototype has been tested in both laboratory and real magnetic resonance (3T) environments.

To demonstrate the functionality of the respiratory triggering, the most frequently used 3D sequence for imaging of the biliary tree outlet and pancreatic ducts was selected, wherein the sequence must be strictly respiratory-triggered. The images obtained were subjectively evaluated by senior radiologists who confirmed that these recordings could be used for diagnosis. This part is described in detail in section 4.B.

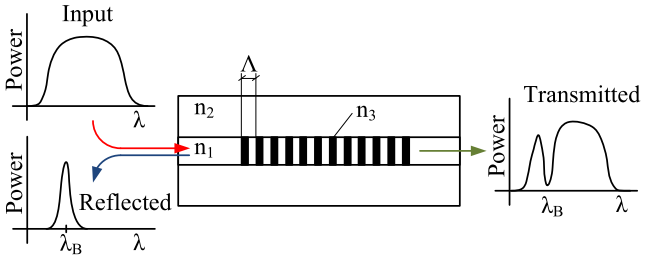

FIGURE 1. The structure of an optical fiber with a bragg grating and its function principle.

III. METHODS

A. FIBER BRAGG GRATING (FBG)

Bragg gratings belong to the category of single-point fiber optic sensors that are used to measure a wide range of physical quantities. The principle of scanning is based on the action of an external deformation or temperature on the optical and mechanical parameters of the grating structure. The Bragg grating structure is formed by the refractive index periodic change in the optical fiber core. When the wide-spectrum light is fed into optical fiber with FBG, a narrow spectral part is reflected from this structure and the other wavelengths pass through the structure without interference, please see Fig. 1. Parameter n_1 denotes the refractive index of the core, parameter n_2 the refractive index of the optical fiber cladding, parameter n_3 the increased refractive index of the optical fiber core.

The central position of the reflection spectrum is called Bragg wavelength and is defined by the following relation:

$$\lambda_B = 2n_{eff}\,\Lambda, \tag{1}$$

where n_{eff} is the effective refractive index of the periodic structure and Λ is the spatial period of the refractive index change. The scanning principles are based on the action of the temperature and the mechanical stress on the periodic structure of the grating. Relation 2 describes the action of deformation and temperature on the change in Bragg wavelength:

$$\frac{\Delta\lambda_B}{\lambda_B} = k\varepsilon + (\alpha_\Lambda + \alpha_n)\,\Delta T, \tag{2}$$

where $\Delta\lambda_B$ is the change in Bragg wavelength, k is the deformation coefficient, ε is the size of deformation, α_Λ is the coefficient of thermal expansion, α_n is the thermo–optic coefficient and ΔT is the change in temperature.

Due to their very small dimensions, Bragg gratings represent an alternative approach to monitoring the vital functions of the human body. As mentioned above, a number of scientific research publications use optical fiber sensors placed on the chest of a human body, implemented in worn fabrics, installed in a mat, backrest, or in bed. This publication represents an innovative version on how to monitor breathing when the Bragg sensor senses the air parameters during inhalation and exhalation via the nasal passage. This approach is particularly suitable for patients who use oxygen inhalation through oxygen glasses.

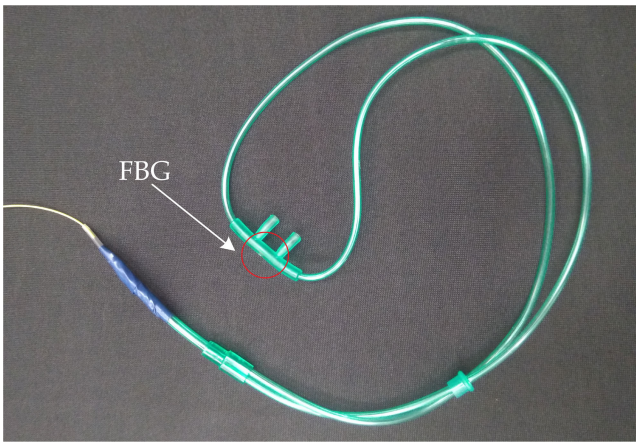

FIGURE 2. A respiration sensor (FOBS) based on encapsulation of FBG into conventional oxygen cannulas.

B. FBG ENCAPSULATION INTO CONVENTIONAL NASAL OXYGEN CANNULAS

The sensor itself is made up of conventional nasal oxygen cannulas, into which an optical fiber with a Bragg grating is fed through a supply tube. The fiber and the FBG are connected to an evaluation unit using G.657.A optical fiber with reinforced protection terminated with an FC/APC connector to eliminate reflections in the couplers. The Bragg grating is set centrally at the inlets that are inserted into nasal cavities. Using an adhesive (Loctite Gel Control), the Bragg grating fiber is fixed at the point of entry into the oxygen cannulas (blue part), see Fig. 2. In the figure, the location of the Bragg grating is marked in red. The Bragg grating portion is not fixed at the point of the outlet of these short tubes (inserting into the nasal cavity). This ensures that the principle of respiratory activity monitoring itself is based on two principles. On the one hand, on the principle of heating or cooling the Bragg grating due to the exhaled or inhaled air, and, on the other hand, on the pressure effect of the exhaled air on the optical fiber with the Bragg grating itself. By the cumulative phenomenon of these two manifestations, the Bragg wavelength and the possibility of respiration monitoring, respiration and exhalation duty cycles, respiratory rate, etc. are influenced.

To implement the FBG, a standard Bragg grating with polyimide recouting with the central Bragg wavelength of 1550.124 nm, the full width at half maximum (FWHM) of the reflected spectrum of 216 nm and the reflectivity of 87 % was used. The encapsulation method has no effect on the mechanical and optical properties of the optical fiber Bragg grating. Sensitivity relations, as well as the central Bragg wavelength, the spectrum width and reflectivity parameters, remain valid, which simplifies the design, manufacture and multiplexing of sensors for monitoring more patients when used for multiple MR scanners.

C. SIGNAL PROCESSING - RESPIRATORY RATE DETERMINATION

The signal processing methodology described below is used to determine the respiratory activity or the respiratory rate,

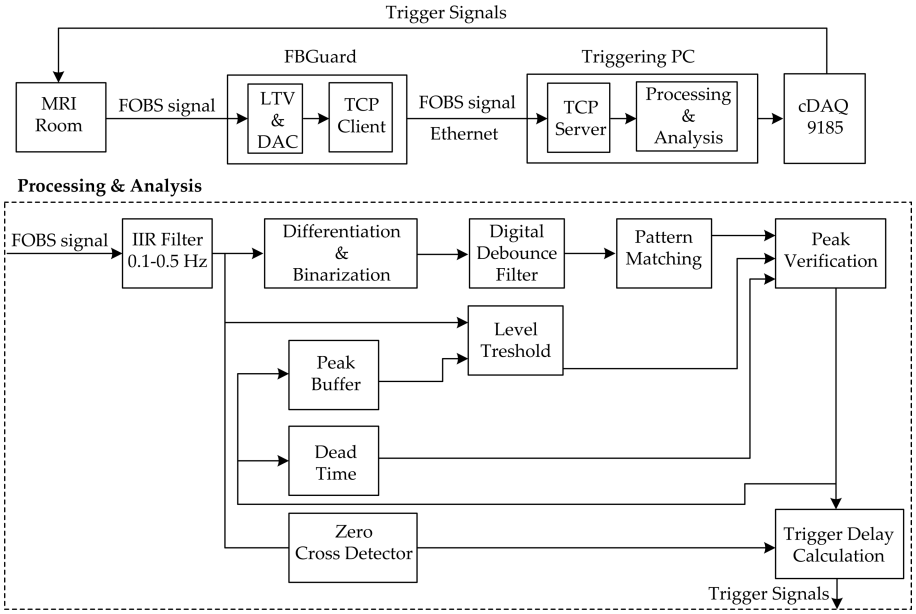

FIGURE 3. A block diagram of the measuring and triggering system used, indicating a detail of processing the signal from FOBS.

respectively. The methodology of respiratory rate determination is coming from our previous research presented in [25], [34] and [35]. The aim of this publication does not bring innovative solutions in the form of signal processing but present the sensor design itself and its functional verification. Input raw signal represents the signal from the used FBG interrogator unit FBGuard (Safibra, Praha, Czech republic). The signal is then filtered to remove any unwanted components formed by motion major artifacts and slow temperature drift by a second-order band-pass Butterworth filter with cut-off frequencies 0.1 and 0.5 Hz. This frequency range corresponds to the typical manifestation of human respiratory activity and eliminates unwanted signal components. In the next step, the signal is processed. This part includes centering, normalization, peak detection and final smoothing of the signal.

Based on detection of the individual peaks (maxima), the respiratory rate (RR) is calculated according to the following equation:

$$RR = 60/\left(t_n - t_{n-1}\right), \tag{3}$$

where t_n is the time mark of the n^{th} peak and t_{n-1} is the time mark of the previous peak.

D. RESPIRATORY TRIGGERING - DESCRIPTION OF SW AND HW IMPLEMENTATION

Signal measurements from FOBS were performed using the FBG monitoring system. It is a fully autonomous system with a built-in PC that allows simultaneous measurement of up to 16 optical channels. The system does not contain digital outputs, so it cannot be used to generate a triggering pulse for magnetic resonance sequence gating. The triggering pulse was generated using a second PC and a CompactDAQ platform made by National Instruments, so this is a system based on virtual instrumentation. The data transfer between the measurement system and the triggering PC was made via the Ethernet interface. The CompactDAQ system is a PC-controlled chassis connectable via Ethernet or USB. The chassis has slots for connecting various input/output modules enabling various sensors, actuators or communication busses to be connected. The cDAQ-9185 system used includes four slots for connecting input/output modules and an Ethernet communication interface. The triggering signal is generated using the cRIO-9472 module (National Instruments, Austin, Texas, USA), which consists of 8 digital outputs, 6 V–30 V compatible, capable of delivering a current of up to 0.75 A per output channel. A more detailed diagram of the entire triggering chain with a detailed examination of signal processing and analysis is shown in the Fig. 3.

The triggering system function is defined by a SW application created in the LabVIEW development environment [36]. The application works as a TCP server connected to the FBGuard system which sends it the optical signal measured sampling a frequency of 1 kHz. The data is sent in packets of 10 values and includes the timestamp of the first sample obtained. The timestamp attached to the data is used to calculate the moment of triggering signal generation. In order to use this timestamp, it was necessary to provide time synchronization between the FBGuard and the triggering PC using a local NTP (Network Timing Protocol) server. The LabVIEW application performs bandwidth filtering of the signal measured using the 2^{nd} order Butterworth approximation with the lower cut-off frequency of 0.1 Hz and the upper cut-off frequency of 0.5 Hz. The signal filtered is then analyzed by a simple positive-peak (inhalations) detection algorithm which works on the principle of signal derivation, its subsequent binarization and the ensuing search for a suitable pattern corresponding to the desired peak. The user can configure the

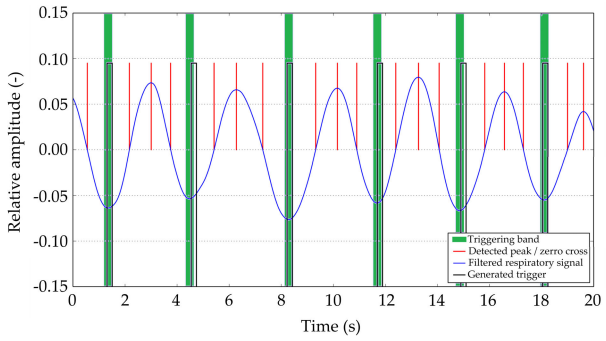

FIGURE 4. Example of trigger pulse generation.

peak detector by defining a so-called dead time (time after the detected peak when the system does not expect a new peak to occur) and a signal level threshold coefficient. Zero-level passages are also detected in the signal, roughly defining the moment at which the inhalation or exhalation is in the middle of its course. Based on the times between the moment of inhalation detected and the respiration signal passage through the zero level, the moment of generating a triggering pulse is calculated.

In order to successfully trigger an MRI sequence, the triggering pulse must be ideally generated at the time the patient finished their exhalation and their ventilation cycle is at a short resting phase. This time interval varies in a window of about 300 to 1000 ms (depending on the respiratory rate and the health state of the person) and, in Fig. 4, it is represented by the light blue band around the negative peak of the respiration waveform filtered. The triggering system determines the moment when the triggering pulse is generated from the moment of passage of the respiration signal filtered through the zero level, i.e. approximately from the middle of the ongoing exhalation. From this moment, the triggering pulse is generated in a time that corresponds to the average of the durations from the middle of the inhalation to the end of the inhalation and from the middle of the inhalation to the end of the exhalation. The triggering pulse time calculation also includes the signal processing time, the signal delay caused by the IIR filter, and the expected delay caused by communication between the triggering PC and the cDAQ system. Fig. 4 depicts a 20 s long section of the respiration signal (blue curve) measured during an ongoing MRI sequence (T2 TSE 3D), showing the moments (vertical red line segments) of the positive peak (inhalation) detected and the signal passages through the zero level. Fig. 4 also shows a generated triggering pulse (black rectangular pulse) with a width of 200 ms, whose beginning is always in the aforementioned triggering band.

IV. EXPERIMENTAL SETUP AND RESULTS

A. RESPIRATORY RATE MEASUREMENTS

The FOBS was initially tested in an experimental laboratory environment (laboratory of VSB-Technical Univ. of Ostrava, Czech republic). This was followed by a series of measurements in a real magnetic resonance environment with a magnetic field of 3T (Siemens Prisma 3T MRI Scanner, Los Angeles, USA) within a multimodal and functional imaging laboratory (CEITEC - Research Centre on Life Sciences, Advanced Materials and Technologies, Brno, Czech republic). In our study, a pneumatic elastic respiratory transducer (type TSD221-MRI), was used as a reference for laboratory environment; in real MRI environment, a respiration MR elastic belt (Siemens Prisma 3T), both for thoracic and abdominal placement, was used. Respiratory belts are further marked with the acronym PRR (pneumatic respiration references). One to two respiration belts in the thoracic and abdominal wall areas are used as a standard as recommended by the manufacturer; it is common medical practice. The measurements were conducted on a sample of 10 healthy volunteers upon their written consent. The age group of the volunteers was from 23 to 57 years and their weight was from 48 to 113 kg. The group of volunteers consisted of 7 men and 3 women. In the laboratory environment, a total of 6 test subjects (4 males and 2 females) were tested, while 4 test subjects (3 males and 1 female) were tested in the real MRI environment. Tab. 1 presents the baseline characteristics of the ten study volunteers. The range is defined by the mean value, maximum and minimum values.

TABLE 1. Baseline characteristics of the ten volunteers taking part in the study.

Subject parameters	Range
Age (years)	40±17
Females n(%)	3(30)
Males n(%)	7(70)
Height (cm)	167±17
Weight (kg)	73±19
BMI (kg/m^2)	25.6±2.8
Systolic blood pressure (mmHg)	119±24
Diastolic blood pressure (mmHg)	69±12

A spectral conventional instrument called FBGuard was used to evaluate the data from the FOBS. We used this type of interrogator unit in our previous research [25] and [35]. Below we described the basic specifics used in this research, which were used again because it was properly validated in our past experiments and the articles. The wavelength resolution of this instrument is 1 pm, the output power is 1 mW and used sampling rate was 1 kHz.

We employed the most widely used Bland-Altman method as a statistical tool for data comparison [37]. Bland-Altman method calculates the mean difference between two methods (respectively instruments - sensors) of measurement, and 95 % limits of agreement as the mean difference ±1.96 SD range. Fig. 5 shows schematically the measurement diagram. In the case of MRI, the FBG interrogator was placed in the control room; we used a standard 6 m long fiber-optic cable (SMF, ITU-T, G.657.A) to connect the interrogator unit and the FOBS. In the laboratory environment, the same type of cable and methodology was used.

A photograph from an experimental measurement in the laboratory environment is shown in Fig. 6(left), a photograph

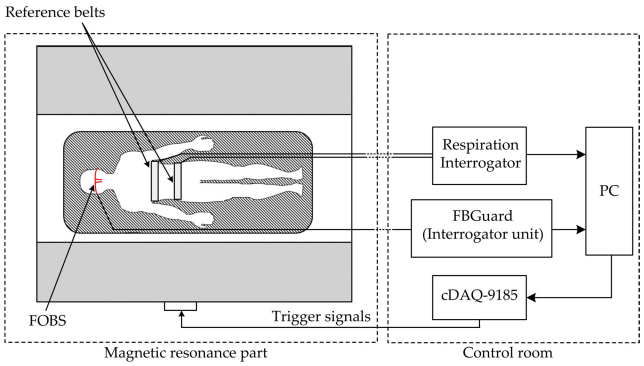

FIGURE 5. Schematic diagram of the experimental measurement.

FIGURE 6. A photo from an experimental measurement in the laboratory environment (left); A photo from the real MR environment (right).

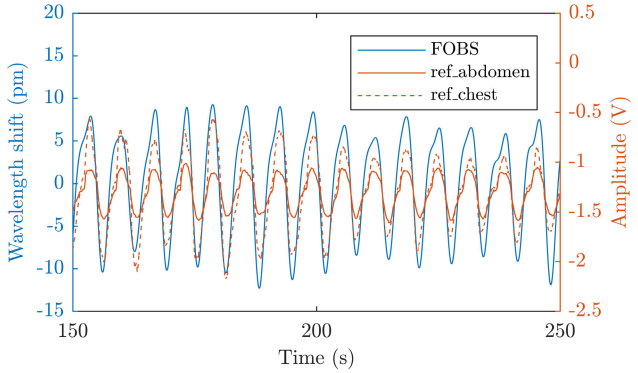

FIGURE 7. A detail of the graphical waveform of respiratory activity obtained from the prototype FOBS having a length of 300 s and detail of signals obtained from reference respiration belts located in the thoracic and abdominal areas (test subject Male1).

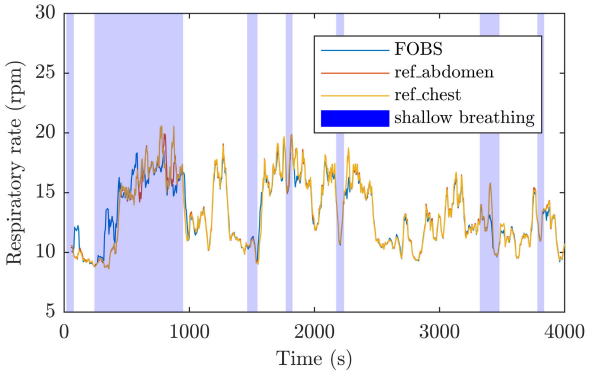

FIGURE 8. An example of the graphical waveform of respiratory rate measurement on a male test subject in a laboratory environment (Male1).

from the real MR environment is shown in Fig. 6(right). The FOBS can be identified in both photos in green (nose placement).

Fig. 7 shows a detail in the form of an example of the graphical waveform of respiratory activity obtained from the prototype FOBS having a length of 300 s (test subject Male1). The study performed has shown that the FOBS allows obtaining dynamic strains on the sensing FBG in the range of 16–31 pm caused by breathing, which is fully measurable by today's FBG interrogation systems, or the FBG interrogator unit used. Fig. 7 also shows a detail of signals obtained from reference respiration belts located in the thoracic and abdominal areas. It is evident that the respiration activity curve has a greater amplitude, which is caused by deepened breathing. This is often seen in patients focusing on respiration activity and may be a problem for the monitoring type recommended by the manufacturer. The signal from the FOBS is inverse towards the reference measurement bands. Exhalation from the nose of the test subject causes the Bragg grating to heat up and, in a full exhalation state, the signal reaches the concave peak while the signals from the reference bands reach the convex peak in this state. In order to graphically compare the signals from FOBS and the reference bands, the FOBS signal was inverted.

Fig. 8 shows an example of the graphical waveform of respiratory rate measurement on a male test subject (Male1) in a laboratory environment against the above–stated respiration reference in the thoracic and abdominal areas. The length of the recording was 66 minutes and 38 seconds. The waveform recorded by the FOBS is shown by the blue curve, the reference respiration curve obtained from the thoracic area is indicated by the yellow curve and the reference respiration curve obtained from the abdominal wall area is indicated by the yellow curve.

Visually, there is a very similar trend of the FOBS to the respiration reference; we can also see that the respiration reference belts themselves differ slightly in their waveforms. This may be caused by a tightened respiration belt and points to the negatives of this measurement method.

Fig. 9 shows the deviation of the RR obtained from FOBS in relation to the reference band located on both the chest and the abdomen. The data measured shows that the average deviation in the time interval of 4000 seconds is 0.41 rpm. In the Fig. 9, the largest deviations are indicated with the blue area. These major errors are caused by shallow breathing, during which the response of the chest and the air exhaled by the nose is different. In fact, this is not a significant problem because the error during shallow breathing is about ± 4 rpm.

Fig. 10 shows a graphical example of a Bland-Altman analysis of the FOBS prototype used against the reference

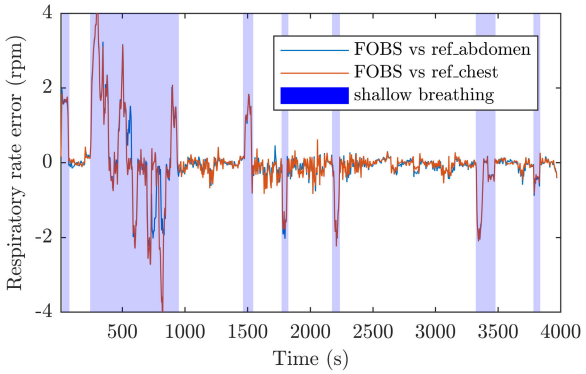

FIGURE 9. Depiction of the deviation of the respiratory rate between FOBS and the reference bands (both thoracic and abdominal placement) - laboratory environment (Male1).

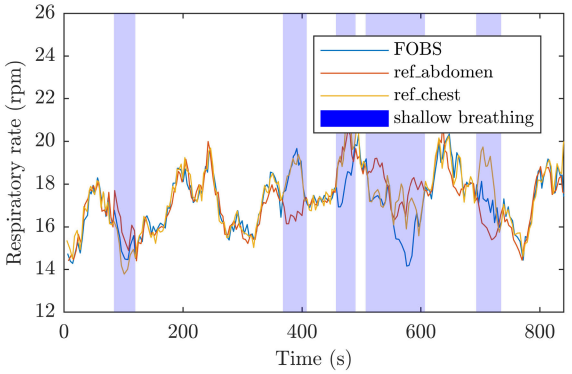

FIGURE 11. An example of the graphical waveform of respiratory rate measurement on a male test subject (Male5) in a real MRI environment (3T MR scanner).

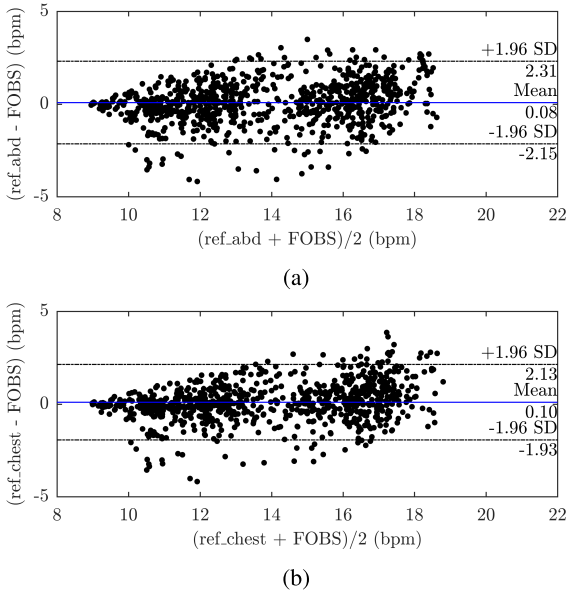

FIGURE 10. Bland-Altman graph: (a) FOBS vs PRR-abdomen (Male1); (b) FOBS vs PRR-chest (Male1).

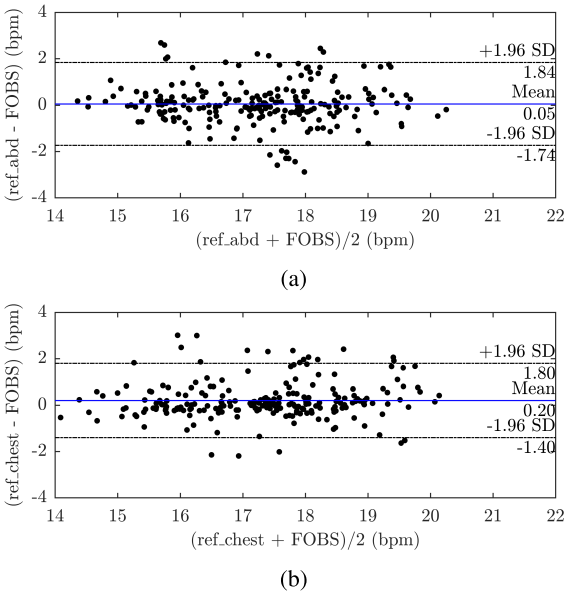

FIGURE 12. Bland-Altman graph: (a) FOBS vs PRR -abdomen (Male5); (b) Bland-Altman graph: FOBS vs PRR -chest (Male5).

respiratory belts for the above-stated test subject recording (Male1) in a laboratory environment. Fig. 10(a) shows a Bland-Altman graph for the FOBS against the respiration reference PRR located in the abdominal area, Fig. 10(b) shows a Bland-Altman graph for the FOBS against the PRR located in the thoracic area. A more detailed statistical analysis is shown in Table 2.

Fig. 11 shows an example of the graphical waveform of respiratory rate measurement on a male test subject (Male5) in a real MRI environment (3T MR scanner) against the PRR in the thoracic and abdominal wall areas. The length of the recording was 13 minutes and 49 seconds (T2 space - brain sequence).

Fig. 12 shows a graphical example of a Bland-Altman analysis of the FOBS prototype used against the reference respiratory belts for the above-stated test subject recording (Male5) in a real MRI environment. Fig. 12(a) shows a Bland-Altman graph for the FOBS against the PRR located in the abdominal area, Fig. 12(b) shows a Bland-Altman graph for the FOBS against the PRR located in the thoracic area. A more detailed statistical analysis is shown in Tab. 3.

Individual parameters of used sequences in MR are shown in Tab. 2.

A summary of the respiratory measurements (laboratory and real MR) is provided in the Tab. 3 and Tab. 4 bellow. Tab. 3 represents data from the laboratory measurements, and Tab. 4 represents data from the MRI measurements. Tables also show data against both used respiratory belts (chest and abdomen). The gender of the subjects tested is displayed as Male1 to Male7 and Female1 to Female3. Tables Tab. 3 and Tab. 4 includes the total recording time (Time), the average respiratory rate (ARR) expressed in respiration per minute (rpm), the total number of the samples recorded by the FOBS (NoS), mean differences (MD), limits of agreement (LoA), which estimate the interval ± 1.96 SD within which a 95 % of the differences between

TABLE 2. Individual parameters of used MRI sequences.

Sequence type	Field of view (mm)	Resolution (px)	Time to echo (ms)	Time to repeat (ms)	Acquisition time (mim:sec)	Flip angle (deg)	Inversion time (ms)	Slice thicknes (mm)
T2-MRCP sequence - T2 triggered bile ducts	379×379	192×256 calculated 752×768	714	1350	3:24	45	-	2
T2 space - brain	224×224	224×224	147	2000	13:49, 12:35	(auto)	-	1mm × 160
T2 space Flair - brain	224×224	224×224	393	5000	8:32, 14:35	(auto)	1800	1mm × 160

TABLE 3. Summary data of the laboratory measurements.

				Chest			Abdomen		
Subject	Time (s)	ARR (rpm)	NoS (-)	MD (rpm)	LoA span (rpm)	Samples in LoA (%)	MoD (rpm)	LoA span (rpm)	Samples in LoA (%)
Male1	3998	15.1	998	0.101	4.067	95.39	0.081	4.453	95.69
Male2	3420	13.3	763	0.092	3.890	96.07	0.077	4.311	96.20
Male3	3515	15.7	911	0.109	4.225	95.28	0.088	4.502	95.61
Male4	3153	12.8	685	0.117	4.413	95.33	0.093	4.617	95.77
Female1	2620	13.4	577	0.089	4.002	96.01	0.084	4.399	96.36
Female2	2883	14.2	664	0.121	4.366	95.78	0.087	4.486	95.93
Summary	19589	-	4598	-	-	-	-	-	-

TABLE 4. Summary data of the MRI measurements.

				Chest			Abdomen		
Subject	Time (s)	ARR (rpm)	NoS (-)	MD (rpm)	LoA span (rpm)	Samples in LoA (%)	MoD (rpm)	LoA span (rpm)	Samples in LoA (%)
Male5	829	17.5	239	0.197	3.203	95.40	0.049	3.573	95.82
Male6	755	15.3	189	0.212	3.410	95.77	0.055	3.722	96.83
Male7	512	15.9	148	0.154	3.119	95.95	0.048	3.284	96.62
Female3	875	15.0	215	0.188	3.487	95.35	0.069	3.477	95.81
Summary	2971	-	791	-	-	-	-	-	-

measurements should lie and the number of differences lying in LoA (±1.96 SD range) expressed as a percentage (Samples in LoA).

The data measured were statistically evaluated using the objective Bland-Altman method and the functionality of the proposed FOBS was confirmed. In the case of laboratory measurements: 95.64 % against reference respiratory belt (chest placement) and 95.93 % against reference respiratory belt (abdomen placement). In the case of MRI measurements: 95.61 % against reference respiratory belt (chest placement) and 96.27 % against reference respiratory belt (abdomen placement). A total relative error (< 5 %) was recorded in all measurements. We can confirmed above-mentioned that the respiration reference belts themselves differ slightly in their waveforms. As we mentioned this may be caused by a tightened respiration belt and points to the negatives of this measurement method.

B. RESPIRATORY TRIGGERING

To confirm the functionality in terms of using FOBS for respiration triggering, the most frequently used sequence for imaging of the biliary tree outlet and pancreatic ducts was selected, wherein the sequence must be strictly respiratory-triggered to eliminate movement artifacts. The images from MRI are shown below; the image obtained using FOBS is displayed in the Fig. 13(a) and the image obtained from the reference respiratory belt (Siemens Prisma 3T) is shown in the Fig. 13(b).

Fig. 13 shows MIP (Maximum Intensity Projection) reconstruction from a T2 weighted sequence for MRCP (Magnetic Resonance Cholangio-Pancreatography) made by a T2 weighted respiratory-triggered 3D sequence. The images in Fig. 13 are made with the same male test subject (Male 5) at virtually the same time (both measurements were performed consecutively). It is possible to differentiate T2 weighted hypersignal structures of the biliary tree and the biliary duct. When using FOBS, the image quality is at least equally good, and even better from the subjective perspective of senior radiologists; a higher contrast between the T2 hypersignal fluid and the environment can be observed (branching of secondary bile ducts, sharp border of duct choledochal). In terms of subjective views of radiologists, both sequences are useful for diagnosis.

Fig. 14 shows a comparison of the T2 weighted image in MIP reconstruction from the sequence of the T2 weighted MRCP imaging triggered with the Male6 male test subject (both measurements were performed immediately after each other). It is possible to differentiate the liquid filling of the biliary tree, the small intestine as well as the kidney outlet system (ren arcuatus). On the right side of the image obtained using a standard Siemens respiratory trigger (trigger period 4.0 s, accept pos. 0 %, SHIFT: H:4.5 mm), the negative effect

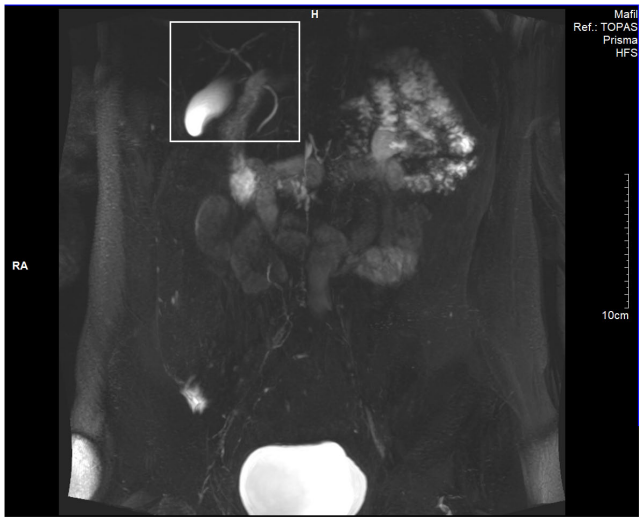

(a)

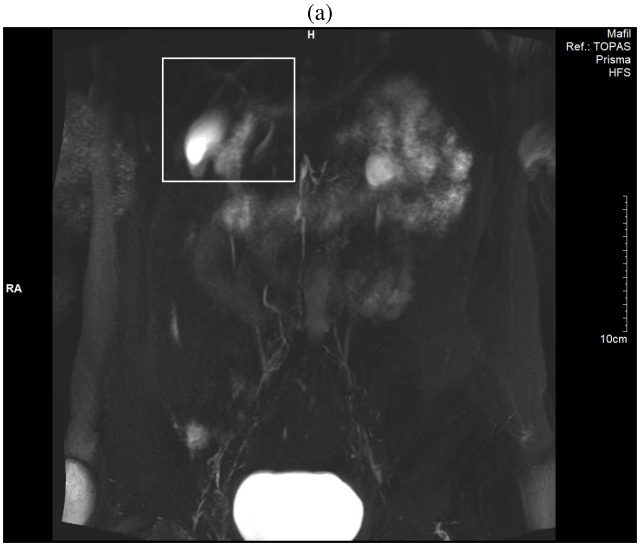

(b)

FIGURE 13. (a) Image obtained by FOBS (Male5). (b) Image obtained by Siemens Prisma 3T respiratory reference (Male5).

of the movement artifact during the movement of the colon sigmoideum can be observed - it may have caused a slight motion blur in the image; higher contrast of the recording may be observed when using FOBS (higher sharpness of the boundaries of the bile ducts and their filling with fluid). In terms of subjective views of radiologists, both sequences are again useful for diagnosis.

In addition to the subjective view of radiologists, the quality assessment of images from MRI was also carried out by software quality analysis using the Blind/Referenceless Image Spatial Quality Evaluator (BRISQUE) [38]. The output of this method is a numerical quality score, which takes values from 0 (best) to 100 (worst). Quality analysis was performed for Fig. 13(a), 13(b), 14(a), and 14(b). In addition to analyzing the overall images, we provided an analysis of the cropped part of the images that were interesting for doctors (white squares). The Quality Score is shown in Tab. 5. The results of image quality analysis show that in all cases

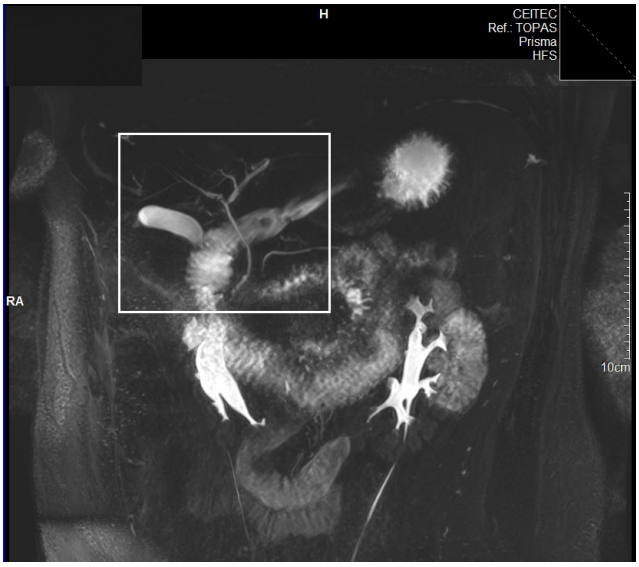

(a)

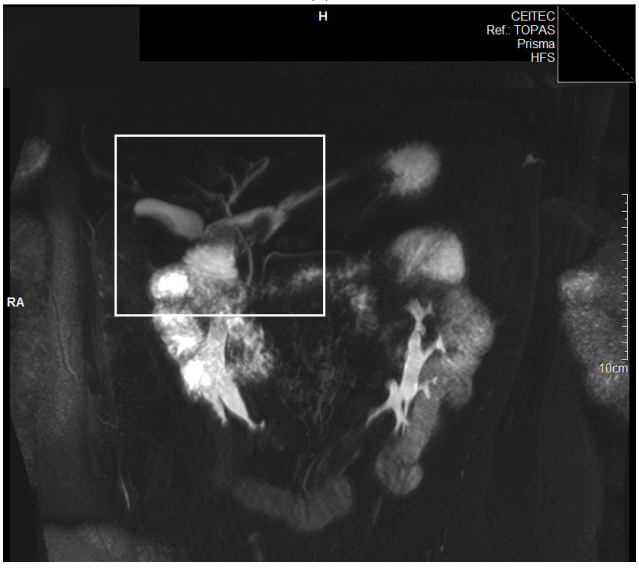

(b)

FIGURE 14. (a) Image obtained by FOBS (Male6). (b) Image obtained by Siemens Prisma 3T Respiratory Reference (Male6).

TABLE 5. Summary data of score quality images. (BRISQUE).

	Fig. 13		Fig. 14	
	(a)	(b)	(a)	(b)
whole image	**46.584**	47.799	**30.883**	31.924
cropped part	**51.763**	55.856	**24.853**	31.096

during the respiratory triggering was achieved by the FOBS equivalent or better image quality.

V. DISCUSSION

This article is focused on the description, laboratory verification and experimental verification of an original and simple low-cost MR fully-compatible and safe sensor based on the FBG in a real MRI environment (after consultation with

senior doctors Pavla Hanzlikova, M.D., Ph.D. and Assoc. prof. Petr Krupa, M.D., Ph.D.) that can be used for monitoring the development of respiratory rate within an MR environment as well as in sleep laboratories, but also in other hospital settings. The FOBS is created by innovative encapsulation of the Bragg grating into conventional oxygen cannulas.

The authors see the benefits in the presentation of the FOBS that is immune to random patient movements. Thanks to this fact, it can be used for the retrospective/ prospective gating within functional MRI (fMRI) and diffuse data (DWI measurement - Diffusion Weighted Imaging, DTI - Diffusion tensor imaging) on the breathing effect, as well as for respiratory triggering. The FOBS was practically verified in a 3T magnetic field; since it uses a combination of pure fiber-optic technology and conventional oxygen cannulas, it is immune to electromagnetic interference (EMI) and its use in any magnetic field (3T and 7T) can be assumed.

However, the basis for using this type is the need for the patient to breathe simultaneously through the mouth and the nose, or just through the nose. Sensor testing was performed on 10 test subjects that were asked to meet the aforementioned condition. No subject had a problem meeting this condition.

In the case of mass production, the price of a complete sensor would be based on many factors that we are currently unable to quantify. Here is the price of the prototype sensor, which includes only the price for the Bragg grating and oxygen cannulas and can be estimated for about 30-40 dollars (work is not included). Although the FBG interrogation unit, which is required for signal evaluation, is a costlier device, it is possible to use the spectral evaluation approach and, using a single FBG interrogation unit, to evaluate units to dozens of sensors. Due to an affordable price, it can be assumed that this type of sensor would be used once. However, there is also a possibility of repeated use in case of sufficient sensor disinfection.

The FOBS is characterized according to the Bland-Altman analysis with an accuracy that is greater than 95 % and a relative error below 5 %. Here, too, the team of authors sees the benefits of the FOBS introduced so far. Now, the approval from the Ethics Committee, which conducted extensive research to identify and analyze the sensor on the largest possible sample of test subjects under clinical practice supervision, is being awaited.

At present, the patient's respiratory cooperation is a prerequisite when displaying the thoracic and abdominal organs. However, most patients are at an age where repeated breath retention for more than 15 seconds leads to early exhaustion and loss of cooperation. This results in a reduced quality of the images obtained, which are often impaired by motion and are therefore minimally usable for diagnosis. From a medical point of view, the development of sequences that allow the patient's free respiration activity is a huge benefit for the future. Based on the reliable measurement of the respiration activity, the sequences that can match the data acquisition with the minimal movement of the diaphragm and the thoracic wall can be developed in the future. This will make the MR examination more accessible to patients with limited cooperation who may benefit from the examination conducted. This alternative respiration monitoring system facilitates the required data acquisition and makes the acquisition more precise, works reliably even in high MR fields, this is promise of the development of other sequences that are now not fully beneficial with partially collaborating subjects.

The possibility of secondary retrospective/prospective filtration of respiratory and cardiac artifacts arising during the measurement of functional MR and diffusion weighted images promises improvement of the output of these measurements, especially in the field of neurosurgery–refining the localization of functional brain centres, more accurate course of neural pathways, this may have a great future benefit in the treatment of brain tumours, but also, for example, in the treatment of epilepsy or mental illness.

VI. CONCLUSION

This publication describes an original MR fully-compatible and safe fiber Bragg grating sensor, which can be used to respiratory triggering and to monitor the development of respiratory rate also within the MR environment. The basic prerequisite is the use of the sensor as prevention of the hyperventilation syndrome commonly found in patients undergoing MR examination. The sensor is created by encapsulation of the Bragg grating into conventional oxygen cannulas. The sensor is immune to random patient movements (minor movements), thus limiting movement artifacts to a minimum. Thanks to this fact it can be used for the retrospective/prospective respiratory gating. The sensor prototype has been tested in both laboratory and real magnetic resonance (3T) environments relative to conventional pneumatic respiration references. The data measured (a relative error under 5 %) were statistically evaluated using the objective Bland-Altman method (> 95 %) and the functionality of the proposed solution was confirmed. Further, Respiratory Triggering functionality was confirmed by the radiologic doctors on the basis of analyzing images using the most used respiratory T2 TSE 3D sequences and by objective method using the Blind/Referenceless Image Spatial Quality Evaluator (BRISQUE).

ETHICS STATEMENT

Ref. No.: EKV-2018-010 Project Title: MR imaging sequences and protocols optimization aiming to the application of new coil and pulse sequences Proposal: 0319/2018 Investigator: Lubomir Vojtisek, Ph.D. Organizational Unit: CEITEC The Research Ethics Committee of Masaryk University has reviewed the application to conduct the research project as specified above and on 8 June 2018 the Committee has approved this project to be conducted

REFERENCES

[1] M. Weckesser, S. Posse, U. Olthoff, L. Kemna, S. Dager, and H.-W. Müller-Gärtner, "Functional imaging of the visual cortex with bold-contrast MRI: Hyperventilation decreases signal response," *Magn. Reson. Med.*, vol. 41, no. 1, pp. 213–216, 1999.

[2] N. D. Giardino, S. D. Friedman, and S. R. Dager, "Anxiety, respiration, and cerebral blood flow: Implications for functional brain imaging," *Comprehensive Psychiatry*, vol. 48, no. 2, pp. 103–112, 2007.
[3] J. G. Webster, "Biomedical instrumentation," in *Handbook of Research on Biomedical Engineering Education and Advanced Bioengineering Learning: Interdisciplinary Concepts*. Hershey, PA, USA: IGI Publishing, 2012, pp. 339–355.
[4] A. Robson, "Dyspnoea, hyperventilation and functional cough: A guide to which tests help sort them out," *Breathe*, vol. 13, no. 1, pp. 45–50, 2017.
[5] C. Rotariu, C. Cristea, D. Arotaritei, R. G. Bozomitu, and A. Pasarica, "Continuous respiratory monitoring device for detection of sleep apnea episodes," in *Proc. IEEE 22nd Int. Symp. Design Technol. Electron. Packag. (SIITME)*, Oct. 2016, pp. 106–109.
[6] J.-W. Yoon, Y.-S. Noh, Y.-S. Kwon, W.-K. Kim, and H.-R. Yoon, "Improvement of dynamic respiration monitoring through sensor fusion of accelerometer and gyro-sensor," *J. Elect. Eng. Technol.*, vol. 9, no. 1, pp. 334–343, 2014.
[7] A. R. Fekr, M. Janidarmian, K. Radecka, and Z. Zilic, "A medical cloud-based platform for respiration rate measurement and hierarchical classification of breath disorders," *Sensors*, vol. 14, no. 6, pp. 11204–11224, 2014.
[8] G. H. Glover, "Overview of functional magnetic resonance imaging," *Neurosurg. Clin.*, vol. 22, no. 2, pp. 133–139, 2011.
[9] P. Podbreznik, D. Onlagic, D. Lesnik, B. Cigale, and D. Zazula, "Cost-efficient speckle interferometry with plastic optical fiber for unobtrusive monitoring of human vital signs," *J. Biomed. Opt.*, vol. 18, no. 10, 2013, Art. no. 107001.
[10] F. C. Favero, J. Villatoro, and V. Pruneri, "Microstructured optical fiber interferometric breathing sensor," *J. Biomed. Opt.*, vol. 17, no. 3, 2012, Art. no. 037006.
[11] S. Sprager, D. Donlagic, and D. Zazula, "Estimation of heart rate, respiratory rate and motion by using optical interferometer as body sensor," in *Proc. IASTED Int. Conf. Signal Image Process. (SIP)*, 2011, pp. 280–287.
[12] S. Sprager, A. Holobar, and D. Zazula, "Feasibility study of heartbeat detection from optical interferometric signal by using convolution kernel compensation," in *Proc. Int. Conf. Bio-Inspired Syst. Signal Process. (BIOSIGNALS)*, 2013, pp. 396–400.
[13] S. Šprager and D. Zazula, "Detection of heartbeat and respiration from optical interferometric signal by using wavelet transform," *Comput. Methods Programs Biomed.*, vol. 111, no. 1, pp. 41–51, 2013.
[14] D. Zazula and S. Šprager, "Detection of the first heart sound using fibre-optic interferometric measurements and neural networks," in *Proc. 11th Symp. Neural Netw. Appl. Elect. Eng. (NEUREL)*, Sep. 2012, pp. 171–176.
[15] S. Šprager, D. Đonlagić, and D. Zazula, "Monitoring of basic human vital functions using optical interferometer," in *Proc. Int. Conf. Signal Process. (ICSP)*, Oct. 2010, pp. 1–4.
[16] J. Nedoma, M. Fajkus, S. Kepak, J. Cubik, S. Zabka, R. Martinek, V. Slany, and J. Marecek, "An interferometric sensor for monitoring respiratory and heart rate of the human body," in *Proc. IEEE 20th Int. Conf. e-Health Netw., Appl. Services (Healthcom)*, Sep. 2018, pp. 1–5.
[17] J. Mathew, Y. Semenova, and G. Farrell, "A miniature optical breathing sensor," *Biomed. Opt. Express*, vol. 3, no. 12, pp. 3325–3331, 2012.
[18] M. Krej, P. Baran, and Ł. Dziuda, "Detection of respiratory rate using a classifier of waves in the signal from a FBG-based vital signs sensor," *Comput. Methods Programs Biomed.*, vol. 177, pp. 31–38, Aug. 2019.
[19] R. Correia, S. James, S. W. Lee, S. P. Morgan, and S. Korposh, "Biomedical application of optical fibre sensors," *J. Opt.*, vol. 20, no. 7, 2018, Art. no. 073003.
[20] H. Su, I. I. Iordachita, J. Tokuda, N. Hata, X. Liu, R. Seifabadi, S. Xu, B. Wood, and G. S. Fischer, "Fiber-optic force sensors for MRI-guided interventions and rehabilitation: A review," *IEEE Sensors J.*, vol. 17, no. 7, pp. 1952–1963, Jan. 2017.
[21] L. Dziuda, J. Lewandowski, F. Skibniewski, and G. Nowicki, "Fibre-optic sensor for respiration and heart rate monitoring in the MRI environment," *Procedia Eng.*, vol. 47, pp. 1291–1294, Jan. 2012.
[22] J. Witt, F. Narbonneau, M. Schukar, K. Krebber, J. De Jonckheere, M. Jeanne, D. Kinet, B. Paquet, A. Depre, L. T. D'Angelo, T. Thiel, and R. Logier, "Medical textiles with embedded fiber optic sensors for monitoring of respiratory movement," *IEEE Sensors J.*, vol. 12, no. 1, pp. 246–254, Jun. 2012.
[23] L. Dziuda, M. Krej, and F. W. Skibniewski, "Fiber Bragg grating strain sensor incorporated to monitor patient vital signs during MRI," *IEEE Sensors J.*, vol. 13, no. 12, pp. 4986–4991, Aug. 2013.
[24] L. Dziuda and F. W. Skibniewski, "A new approach to ballistocardiographic measurements using fibre Bragg grating-based sensors," *Biocybern. Biomed. Eng.*, vol. 34, no. 2, pp. 101–116, Jan. 2014.
[25] J. Nedoma, M. Fajkus, R. Martinek, and H. Nazeran, "Vital sign monitoring and cardiac triggering at 1.5 Tesla: A practical solution by an MR-ballistocardiography fiber-optic sensor," *Sensors*, vol. 19, no. 3, p. 470, 2019.
[26] A. G. Leal-Junior, C. R. Díaz, C. Leitão, M. J. Pontes, C. Marques, and A. Frizera, "Polymer optical fiber-based sensor for simultaneous measurement of breath and heart rate under dynamic movements," *Opt. Laser Technol.*, vol. 109, pp. 429–436, Jan. 2019.
[27] L. Dziuda, "Fiber-optic sensors for monitoring patient physiological parameters: A review of applicable technologies and relevance to use during magnetic resonance imaging procedures," *J. Biomed. Opt.*, vol. 20, no. 1, 2015, Art. no. 010901.
[28] C. Santelli, R. Nezafat, B. Goddu, W. J. Manning, J. Smink, S. Kozerke, and D. C. Peters, "Respiratory bellows revisited for motion compensation: Preliminary experience for cardiovascular MR," *Magn. Reson. Med.*, vol. 65, no. 4, pp. 1098–1103, 2011.
[29] A. C. Larson, P. Kellman, A. Arai, G. A. Hirsch, E. McVeigh, D. Li, and O. P. Simonetti, "Preliminary investigation of respiratory self-gating for free-breathing segmented cine MRI," *Magn. Reson. Med.*, vol. 53, no. 1, pp. 159–168, 2005.
[30] B. Hiba, N. Richard, M. Janier, and P. Croisille, "Cardiac and respiratory double self-gated cine MRI in the mouse at 7 T," *Magn. Reson. Med.*, vol. 55, no. 3, pp. 506–513, 2006.
[31] A. C. S. Brau, C. T. Wheeler, L. W. Hedlund, and G. A. Johnson, "Fiber-optic stethoscope: A cardiac monitoring and gating system for magnetic resonance microscopy," *Magn. Reson. Med.*, vol. 47, no. 2, pp. 314–321, 2002.
[32] A. Rengle, L. Baboi, H. Saint-Jalmes, R. Sablong, and O. Beuf, "Optical cardiac and respiratory device for synchronized MRI on small animal," in *Proc. Annu. Int. Conf. IEEE Eng. Med. Biol.*, Aug. 2007, pp. 2046–2049.
[33] C. B. Saw, E. Brandner, R. Selvaraj, H. Chen, M. S. Huq, and D. E. Heron, "A review on the clinical implementation of respiratory-gated radiation therapy," *Biomed. Imag. Intervent. J.*, vol. 3, no. 1, p. e40, Jan. 2007.
[34] J. Nedoma, "Magnetic resonance imaging compatible non-invasive fibre-optic sensors based on the Bragg gratings and interferometers in the application of monitoring heart and respiration rate of the human body: A comparative study," *Sensors*, vol. 18, no. 11, p. 3713, 2018.
[35] M. Fajkus, J. Nedoma, R. Martinek, V. Vasinek, H. Nazeran, and P. Siska, "A non-invasive multichannel hybrid fiber-optic sensor system for vital sign monitoring," *Sensors*, vol. 17, no. 1, p. 111, Jan. 2017.
[36] C. Elliott, V. Vijayakumar, W. Zink, and R. Hansen, "National instruments LabVIEW: A programming environment for laboratory automation and measurement," *JALA, J. Assoc. Lab. Automat.*, vol. 12, no. 1, pp. 17–24, Jul. 2007.
[37] J. M. Bland and D. G. Altman, "Measuring agreement in method comparison studies," *Stat. Methods Med. Res.*, vol. 8, no. 2, pp. 135–160, 1999.
[38] A. Mittal, A. K. Moorthy, and A. C. Bovik, "No-reference image quality assessment in the spatial domain," *IEEE Trans. Image Process.*, vol. 21, no. 12, pp. 4695–4708, Dec. 2012.

MARCEL FAJKUS was born in Czech Republic, in 1987. He has been an Assistant Professor with the VSB—Technical University of Ostrava, since 2016. His current research interests include fiber Bragg sensors and distributed systems in traffic, civil engineering, and biomedical applications. He has more than 120 journal and conference papers in his research areas and holds three valid patents.

JAN NEDOMA was born in Czech Republic, in 1988. He received the master's degree in information and communication technology from the VSB—Technical University of Ostrava, in 2014, where he has been a Research Fellow, since 2014. In 2017, he successfully defended his dissertation thesis and is currently an Assistant Professor with the VSB—Technical University of Ostrava. His current research interests include fiber-optic sensors in traffic, civil engineering, and biomedical applications. He has more than 115 journal and conference articles (author h-index: nine without self-citations) in his research areas and holds six valid patents.

RADEK MARTINEK was born in Czech Republic, in 1984. He received the master's degree in information and communication technology from the VSB—Technical University of Ostrava, in 2009, where he has been a Research Fellow, since 2012. In 2014, he successfully defended his dissertation thesis titled "The Use of Complex Adaptive Methods of Signal Processing for Refining the Diagnostic Quality of the Abdominal Fetal Electrocardiogram." He became an Associate Professor in technical cybernetics with the VSB—Technical University of Ostrava, in 2017, after defending the habilitation thesis titled "Design and Optimization of Adaptive Systems for Applications of Technical Cybernetics and Biomedical Engineering Based on Virtual Instrumentation." He has been an Associate Professor with the VSB—Technical University of Ostrava, since 2017. His current research interests include digital signal processing (linear and adaptive filtering, soft computing—artificial intelligence and adaptive fuzzy systems, nonadaptive methods, biological signal processing, and digital processing of speech signals), wireless communications (software-defined radio), and power quality improvement. He has more than 200 journal and conference articles in his research areas.

JINDRICH BRABLIK was born in 1991. He received the bachelor's degree in biomedical technology and the master's degree in information and control systems from the Faculty of Electrical Engineering and Computer Science, VSB—Technical University of Ostrava, where he is currently pursuing the Ph.D. degree in technical cybernetics, with a focus on virtual instrumentation and signal processing of physiological signals.

JAN VANUS graduated in measuring and control engineering from the Faculty of Electronics and Informatics, VSB—Technical University of Ostrava, in 1996, where he has been a Lecturer, since 2001. In 2010, he successfully defended his Ph.D. thesis "Voice Communication with the Control System." Since 2015, he has been a Lecturer with the Department of Cybernetics and Biomedical Technology, VSB—Technical University of Ostrava. His research interests include the design, implementation, and monitoring of operational-technical function management in intelligent buildings.

MARTIN NOVAK was born in Prostejov, Czech Republic, in 1988. He is currently pursuing the Ph.D. degree with the VSB—Technical University of Ostrava. He focused on fiber-optic sensors.

STANISLAV ZABKA was born in Myjava, Slovakia, in 1988. He received the bachelor's and master's degrees in information technologies from the Department of Information and Communications Technologies, Faculty of Electrical Engineering and Computer Science, VSB—Technical University of Ostrava, in 2010 and 2013, respectively, where he is currently pursuing the Ph.D. degree. He is currently a Software Developer with International IT Company in the areas of energy utilities, distribution process, and communication.

VLADIMIR VASINEK was born in Ostrava. He graduated in physics, specialization in optoelectronics, from the Science Faculty, Palacky University, in 1980. He received the Ph.D. degree in quantum electronics and optics, in 1989. He became an Associate Professor in applied physics, in 1994. He has been a Professor of electronics and communication science with the Department of Telecommunications, VSB—Technical University of Ostrava, since 2007. His research work is dedicated to optical communications, optical fibers, optoelectronics, optical measurements, optical networks projecting, fiber optic sensors, and MW access networks. He is a member of many societies, such as OSA, SPIE, EOS, and the Czech Photonics Society. He is the Chairman of the Ph.D. Board with the VSB—Technical University of Ostrava. He is also a member of habitation boards and the boards appointing to professorship. He was awarded the title of RNDr in applied electronics at the Science Faculty, Palacky University.

PAVLA HANZLIKOVA is currently with the Clinic of Imaging Methods of Faculty Hospital, University of Ostrava, Ostrava. She deals with interventional neuroradiology, MR spectroscopy, and interventional applications of 3D image.

LUBOMIR VOJTISEK received the Ph.D. degree in measurement from the Faculty of Electrical Engineering and Information Technology, Slovak Technical University. He is currently a Researcher and a Technical Specialist Member of the Multimodal and Functional Neuroimaging Research Group, Masaryk University, where he is also a Postdoctoral Research Fellow.